CHANGE OF THE MAGNETIC FIELD STRUCTURE DURING RELAXATION IN THE HIGH PINCH PARAMETER REGIME OF THE REVERSED FIELD PINCH REPUTE-1

Y. UEDA*, N. ASAKURA**, S. MATSUZUKA***, K. YAMAGISHI, S. SHINOHARA, Y. NAGAYAMA, H. TOYAMA, K. MIYAMOTO
Department of Physics,
Faculty of Science

N. INOUE
Department of Nuclear Engineering,
Faculty of Engineering

University of Tokyo,
Bunkyo-ku, Tokyo, Japan

ABSTRACT. Magnetic field measurements in a reversed field pinch plasma have been made with an insertable magnetic probe in REPUTE-1. The relaxation process of the magnetic field configuration in a high θ (θ is the pinch parameter) regime has been studied. The safety factor on axis, q_0, decreases as θ increases, and there exists a lower limit to $q_0(\sim 0.10)$. Close to this limit, q_0 increases when the magnetic field configuration relaxes. These observations agree well with numerical results of non-linear resistive MHD theory.

1. INTRODUCTION

The reversed field pinch (RFP) [1], an axisymmetric toroidal system like the tokamak, generates a magnetic field configuration close to the force free minimum energy state given by Taylor [2]. This process, by which the magnetic field in a slightly resistive plasma changes its topology through field line reconnection, is known as 'relaxation'. Recently, field line reconnection driven by MHD kink instabilities has attracted increased attention as the mechanism responsible for the relaxation [3–8]. Caramana et al. [4] calculated the non-linear evolution of the magnetic field structure of an RFP with a single helicity. They showed that the unstable non-resonant kink mode becomes stable when the safety factor on axis, q_0, increases and that the resonant surface is restored after the reconnection. During this process, the magnetic field configuration approaches the minimum energy state, which indicates that this type of reconnection ('inverse reconnection') is one of the relaxation mechanisms. Sato and Kusano [6] gave a physical interpretation of the dynamics of this process, named 'non-linear driven reconnection'. They showed that axial plasma flow induced by the kink instability is the cause of field line reconnection and relaxation. Also Miyamoto analysed the effects of the MHD kink mode on toroidal flux generation with the help of the non-linear driven reconnection model [9]. Since overlapping of magnetic islands at different singular surfaces cannot be neglected in the RFP, three-dimensional MHD simulation is necessary. According to a study by Schnack et al. [5], strong mode coupling of m = 1 to both m = 2 and m = 0 is observed, and magnetic island overlap causes stochastic field lines. In the case of a high pinch parameter, $\theta(>1.6)$, the entire plasma becomes stochastic during relaxation, while for the low $\theta(<1.6)$ case an intact flux surface remains in the outer region.

Experimentally, it is found that a coherent periodic relaxation oscillation with large amplitude appears at relatively high θ. In ZT-40M [10–13], a toroidal flux oscillation showed up with large m = 0 amplitude soft X-ray sawteeth. Similar phenomena have been observed in TPE-1R(M) [14] and ETA-BETA II

* Present address: Faculty of Engineering, Osaka University, Osaka 565, Japan.
** Present address: Plasma Physics Laboratory, Princeton Univ., P.O. Box 451, Princeton, NJ 08544, USA.
*** Present address: Toshiba Corporation, Fuchu, Japan.

[15]. So far, it is uncertain whether these phenomena are caused by the same mechanism since the oscillation appears not only in the current sustainment phase (ZT-40M, ETA-BETA II), but also in the current rise phase (ZT-40M) and around the current peak (TPE-1R(M)). However, there are several features that are common to these observations. First, the oscillation occurs when θ becomes relatively high ($\theta > 1.6$ for ZT-40M and TPE-1R(M), $\theta > 2.0$ for ETA-BETA II). Second, the oscillation is accompanied by a change in the amplitude of the m = 1 magnetic fluctuation at the wall. For example, in ZT-40M, the amplitude of the magnetic fluctuation decreases when the soft X-ray signal decreases. Third, during this process, the toroidal flux and θ also oscillate. The toroidal flux increases and θ decreases when the amplitude of the m = 1 magnetic fluctuation decreases. These results suggest that it is the MHD kink instability that, possibly, is related to the relaxation process of the RFP plasma. However, this process and the relaxation mechanism itself are not sufficiently understood since the time evolution of the magnetic field profile and the change of q_0 during this process are not clear.

This paper presents the results of an experimental study in REPUTE-1 of the relaxation processes taking place in a high θ ($\theta > 1.75$) plasma just before the current peak. The existence of a lower limit to q_0, as reported in Ref. [16], is confirmed, and the m = 0, 10 kHz magnetic field oscillations are interpreted as the results of two alternating processes: current peaking and relaxation. The relaxation process appears to agree satisfactorily with resistive non-linear MHD simulations.

2. EXPERIMENTAL SET-UP

REPUTE-1 is an RFP device with a resistive shell [17], the skin time of which is 1 ms for vertical field penetration. The dimensions of this device are as follows: major radius R = 0.82 m, minor radius (limiter radius) a_{lim} = 0.20 m, and wall radius a_w = 0.22 m. The machine is usually operated in an aided reversal mode.

The magnetic probe system used in the experiment is shown in Fig. 1. The tip of the magnetic probe can approach the plasma centre. The leads from the coils are brought out as a tightly twisted pair, and the signals are transmitted to differential amplifiers to reduce the common mode noise. The magnetic fields in the toroidal and poloidal directions are measured simultaneously at six radial positions 3.4 cm apart. The surface area of each magnetic pickup coil is 6 × 5 mm^2, and the centres of each pair of toroidal and poloidal coils are 3 mm apart. The probe is inserted into a protective alumina jacket, the frequency response of which exceeds 200 kHz, the cut-off frequency of the low pass filter in the differential amplifier (Lecroy 8100). The calibration of the coils is made on the vacuum toroidal field and agrees within 5% with the geometrical estimate. The magnetic probe signals are sampled each microsecond with a CAMAC digital data acquisition system and integrated numerically to obtain the magnetic field strength.

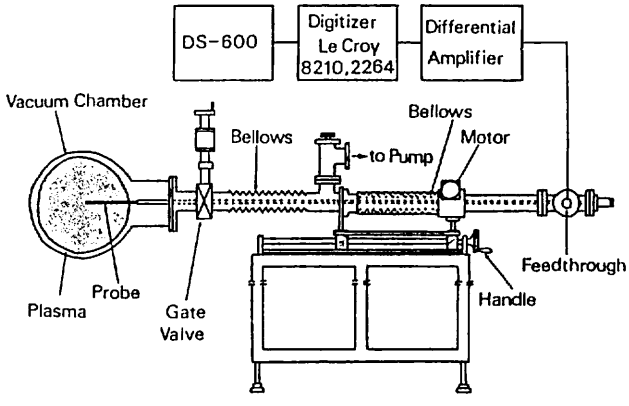

FIG. 1. Schematic view of insertable magnetic probe system.

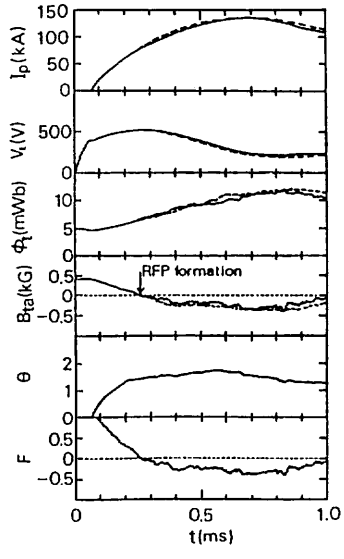

FIG. 2. Time evolution of plasma parameters. Plasma current I_p, one-turn loop voltage V_t, toroidal field at the plasma edge B_{ta}, pinch parameter θ, and reversal ratio F are shown. The dotted lines show the same parameters when no probe was inserted.

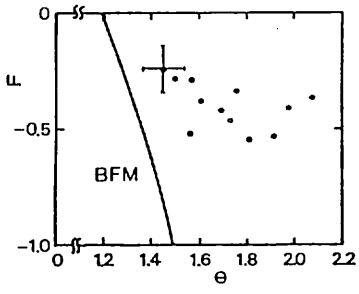

FIG. 3. Discharge regime on F–θ diagram. Solid line shows F–θ value derived from Bessel Function Model.

The time evolution of typical plasma parameters in this experiment is shown in Fig. 2. The peak plasma current is approximately 135 kA at 0.7 ms and the RFP formation time 0.25 ms. The toroidal flux is close to 5 mWb at the initiation of the plasma current and grows up to 10 mWb at the current peak. The line averaged density lies between 0.5×10^{14} and 1.2×10^{14} cm^{-3}. As is shown in Fig. 2, plasma parameters such as plasma current, loop voltage, and magnetic fluctuation level at the plasma edge are not affected by the probe even when it is inserted as far as the plasma centre.

To obtain a high θ plasma at the current peak, a decrease in the external reversed toroidal flux is programmed by the external circuit. The value of F (reversal ratio) tends to decrease as θ increases, as is shown in Fig. 3. Typical F and θ values are $F = -0.3$ and $\theta = 1.6$.

3. DEPENDENCE OF FIELD PROFILES ON THE PINCH PARAMETER

For computations, the toroidal magnetic field, B_t, and the poloidal field, B_p, are approximated by smoothing functions, including a first order toroidal correction. These functions are presented in detail in the Appendix. Figure 4 shows the difference of profiles between low θ (=1.57) and high θ (=1.98) discharges. The position of the magnetic axis normally deviates from the centre of the limiter by 2–3 cm at current peak time. The Shafranov shift Δ is only 0.5–1.0 cm. Therefore, the plasma shifts outward by an additional 2 cm away from the centre of the limiter. In the high θ case, the toroidal current profile is more peaked on axis, and the value of q_0 is smaller than in the low θ case. The profile of λ ($\mu_0 \vec{j} \cdot \vec{B}/B^2$) is nearly

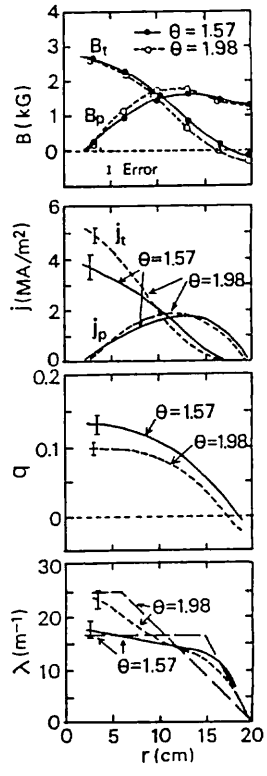

FIG. 4. Field profiles in low θ(=1.57, closed circle and solid line) and high θ(=1.98, open circle and broken line) cases. Toroidal field B_t, poloidal field B_p, toroidal current density j_t, poloidal current density j_p, safety factor q, and $\lambda(\mu_0 \vec{j} \cdot \vec{B}/B^2)$ are shown. Dashed lines show profiles derived from MBFM.

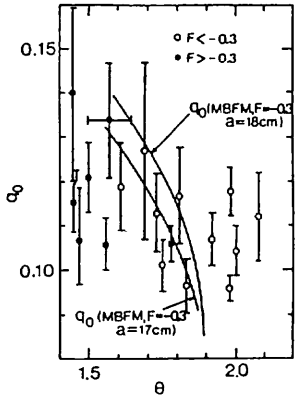

FIG. 5. Safety factor on axis q_0 at the current peak versus pinch parameter θ with the q_0 of MBFM (F = −0.3). Open circles are for F < −0.3 and closed circles are for F > −0.3.

flat except at the plasma edge in the low θ case, and the magnetic field configuration is close to that of the relaxed state. However, in the high θ case the profile of λ is peaked on axis, and the magnetic field configuration is away from the relaxed state. The λ profile calculated from the Modified Bessel Function Model (MBFM) [18] by using experimentally observed F and θ values is also shown. The observed λ profile agrees well with the calculated one. Figure 5 shows the safety factor on axis q_0 as a function of θ and the calculated value from the MBFM (F = −0.3). In the low θ region ($\theta < 1.70$), q_0 scatters between $q_0 = 0.106$ and $q_0 = 0.140$, while in the high θ region ($\theta > 1.70$), q_0 scatters between $q_0 = 0.096$ and $q_0 = 0.118$. The value of q_0 has a tendency to decrease with θ. The experimental data of q_0 (F = −0.3) are close to those of the MBFM. The value of q_0 saturates above $\theta = 1.70$.

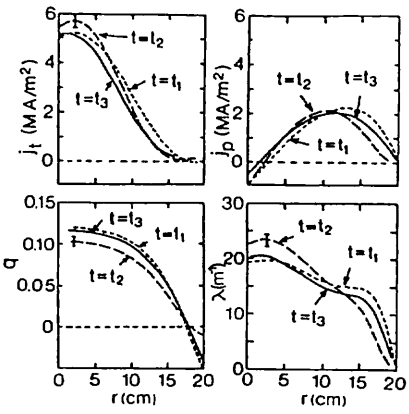

FIG. 7. Change of profiles of toroidal current density j_t, poloidal current density j_p, safety factor q, and λ during relaxation oscillation. Times t_1, t_2, and t_3 are the same as those in Fig. 6.

4. RELAXATION OSCILLATION IN THE HIGH PINCH PARAMETER REGIME

In the previous section, it was shown that q_0 saturates in the high θ regime. In this regime, a relaxation oscillation of the magnetic field in the plasma has been observed just before the current peak as the pinch parameter θ exceeds a value of approximately 1.75;

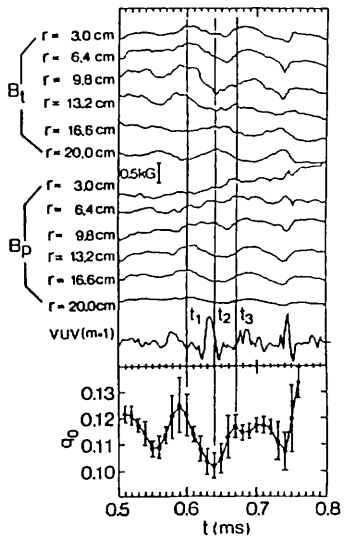

FIG. 6. Time evolution of the magnetic field in the plasma, safety factor on axis q_0, and m = 1 VUV fluctuation (f > 15 kHz) in high θ case ($\theta \sim 1.7$). Poloidal field at r = 3 cm is approximately zero at t = 0.5 ms.

this phenomenon is related to the saturation of q_0. The period of oscillation is about 0.1 ms, and the relative amplitude ($\delta B/B$) is 20% at maximum. The time evolution of the magnetic field, of q_0, and of the m = 1 vacuum ultraviolet (VUV) fluctuations during the oscillation is shown in Fig. 6. The m = 1 component of the VUV fluctuations (f > 15 kHz, obtained by a surface barrier diode) is defined as the difference of two VUV signals emitted from symmetrical positions with respect to the plasma equatorial plane (at ±14 cm). From $t = t_1 = 0.60$ ms to $t = t_2 = 0.64$ ms, the toroidal magnetic field decreases in the central region ($r \leq 13.2$ cm) and increases outside ($r \geq 16.6$ cm), while the poloidal field outside ($r \geq 13.2$ cm) decreases. However, from $t = t_2$ to $t = t_3 = 0.67$ ms, the magnetic field changes the opposite way. Figure 7 shows the change during the oscillation of the profiles of the current, of q, and of λ as obtained from the insertable magnetic probe. From $t = t_1$ to $t = t_2$, q_0 decreases and the toroidal current profile and the λ profile become peaked on axis. From $t = t_2$ to $t = t_3$, conversely, q_0 increases and the profiles approach flat profiles. The values of F and θ are −0.15 and 1.73 at $t = t_2$ and −0.25 and 1.64 at $t = t_3$, which means that the discharge parameters approach that of the relaxed state. These results indicate that the field configuration becomes more relaxed after q_0 has increased. The m = 1 VUV fluctuations decrease after the increase of q_0 ($t \sim 0.70$ ms), which indicates that the m = 1 MHD activity is reduced after the increase of q_0. The rise time of q_0 is shorter than or at least equal to the decay time of q_0 and is less than 40 μs (typically 20 μs). In this discharge the

Alfvén transit time τ_A is approximately 0.7 μs, and the rise time of q_0 is less than 60 $\times$ τ_A (typically 30 $\times$ τ_A).

During the oscillation, the toroidal flux calculated from the magnetic field profile increases, which indicates that this process is a mechanism for toroidal flux generation. The poloidal flux does not always decrease during this process; therefore, from these data it is not clear that flux conversion from poloidal to toroidal flux takes place. Since the oscillation is observed just before the current peak when the plasma current is still rising, this may obscure the flux conversion mechanism. In a few cases, the plasma current measured by a Rogowski loop shows the same kind of oscillation as the internal magnetic field, but often there is no clear correlation. In most cases, the toroidal flux oscillations (measured by an external loop) correlate with those on the internal magnetic field but the phase of the oscillation is not always the same. The locations of the toroidal flux loop and the internal magnetic probe are 90° apart in the toroidal direction, which may affect the results. The magnetic axis of the plasma usually moves toward the major axis around current peak time, known from the increase with time of the poloidal magnetic field at r = 3 cm, even if the oscillations do not take place. Most of the oscillations are accompanied by a rapid shift of the magnetic axis ($\leq$ 1.0 cm) toward the major axis, in addition to the normal shift.

Figure 8 shows the relation between Δq_0 (= q_{0f} − q_{0i}) and q_{0i}. Here q_{0i} is the minimum value of q_0 and q_{0f} is the value of q_0 40 μs after q_0 acquired its minimum. The value of Δq_0 becomes large as q_{0i} decreases below approximately 0.10 (q_{0f} lies between 0.11 and 0.12). This suggests that it is the magnitude of Δq_0 that determines the lower limit of q_0 (~0.10), similar to the sawtooth oscillation of a tokamak internal disruption in the case of q_0 ~ 1.

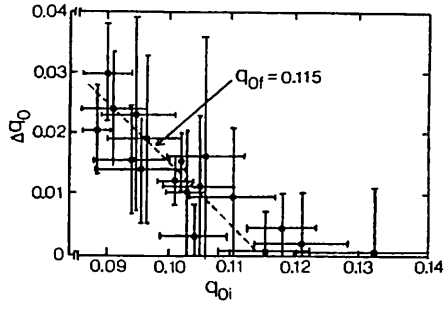

FIG. 8. Amplitude of oscillation of safety factor on axis, $\Delta q_0 (= q_{0f} - q_{0i})$ versus q_{0i}.

5. DISCUSSION

As was shown in Section 3, q_0 saturates as the value of θ is raised above about 1.75. The existence of a q_0 limit has already been pointed out by Ortolani [16], who suggested the scaling q_0 = 2a/3R for the RFP [15]. In REPUTE-1, the same scaling gives 0.14 instead of the measured value of approximately 0.10, which rather suggests the scaling a/2R. When q_0 is reduced to its limit, a relaxation oscillation is observed, which indicates a clear relation between the two phenomena. During the oscillation, the plasma MHD activity changes with q_0: the m = 1 VUV fluctuation decreases when q_0 increases. The toroidal mode number n of the magnetic fluctuation at the plasma edge is measured by two magnetic probes 20° apart in the toroidal direction. The phase difference of the fluctuations on the two magnetic probes (with the same frequency as that of the VUV signal) is about 180°, which indicates a toroidal mode number of 9. The value of q_0 is nearly the same as m/n (~0.11); therefore, the fluctuation appears to be related with the q profile. From our observations, it is, however, difficult to determine whether this mode is resonant or not. According to the model of Caramana et al. [4] the magnetic field profile becomes unstable against the tearing mode (resonant) since the parallel current density increases when the current peaks. By a Kadomtsev type reconnection, the resonant surface is removed and the magnetic field profile becomes unstable against the ideal kink mode (non-resonant). This instability is caused by a decrease in the magnetic shear due to the reduction of q_0. A stabilizing effect (inverse reconnection) then occurs with the increase of q_0, and the relaxation of the magnetic field configuration takes place. From our experimental data, it is not known whether the m = 1 VUV fluctuation is mainly caused by the tearing mode or by the ideal kink mode. But it is clear that the relaxation of the RFP plasma is caused by MHD instability.

Our experimental observations agree well with the numerical results of non-linear resistive MHD simulations [5, 8]. The rise-time of q_0 in these simulations is typically (10−20) $\times$ τ_A, which is consistent with our experimental results (typically 30 $\times$ τ_A). In Ref. [9] it is shown that the toroidal flux can be generated by inverse reconnection when the helicity of the unstable kink mode (m/n) driving the reconnection is close to q_0 and non-resonant before the reconnection. In our experiments, the toroidal flux calculated from the toroidal magnetic field profile increases after q_0. The observed mode helicity (m/n ~ 0.11) is nearly the

TABLE I. COMPARISON BETWEEN OHMIC HEATING TIME τ_{OH} AND OSCILLATION PERIOD τ_{osc}

Device	ZT-40M	ETA-BETAII	TPE-1R(M)	REPUTE-1
I(kA)	120	75	75	130
R(m)	1.14	0.65	0.50	0.82
a(m)	0.20	0.125	0.09	0.20
T_e(eV)	200	—	300	40
V_l(V)	66	~50	50	220
η ($\mu\Omega$·m)	9.6	8	5.4	41
$\tau_{OH} \propto a^2/\eta$(a.u.)	4.2	2	1.5	1.0
τ_{osc}(ms)	~0.7	~0.2	~0.15	~0.1

same as q_0, which is consistent with the theory of Ref. [9].

The relaxation oscillation phase of an RFP plasma in the high θ regime consists of two parts, a current peaking phase and a relaxation phase. In ZT-40(M) [19] and TPE-1R(M) [14], the soft X-ray signal gradually increases during the current peaking phase and rapidly decreases during the shorter relaxation phase. Also in REPUTE-1, the duration of the current peaking phase is longer than or at least equal to that of the relaxation phase. Therefore, the period of the relaxation oscillation is expected to correlate with the current peaking time, as suggested by Werley et al. [19]. At this point, it seems useful to estimate the Ohmic heating time τ_{OH}, which is proportional to the current peaking time. The Ohmic heating time τ_{OH} is calculated from $\beta\tau_R \propto \beta a^2/\eta$, where β is the ratio of plasma pressure to magnetic pressure and η is the plasma resistivity. The results of four RFP devices are shown in Table I. In this calculation, the β values are assumed to be equal since most of the RFP plasmas have nearly the same β_p value (ratio of plasma pressure to poloidal magnetic field pressure, ~10%) and the β value is proportional to β_p for equal pressure profile and magnetic field profile. The calculation reveals a clear correlation between the value of a^2/η and the relaxation oscillation period τ_{osc}. The value of a^2/η is proportional to $RI_p/V_l = R/R_p$, where R_p is the plasma resistance. In ZT-40M, R_p is low and the dimension of the device is large, which is the reason why the period of the relaxation oscillation is the longest. In TPE-1R(M), the short period of the relaxation oscillation, even if the electron temperature is high, is due to the small dimension of the device. In REPUTE-1, the plasma resistance is large, which causes a short period of this oscillation. The results suggest that in all devices the current peaking is caused by a thermal instability [4]. Further study is, however, needed to better understand the relaxation phase of this oscillation, since there are differences in the value of θ above which this oscillation appears ($\theta > 1.6$ for ZT-40M and TPE-1R(M), $\theta > 1.75$ for REPUTE-1, and $\theta > 2.0$ for ETA-BETA II) and in the current behaviour (decaying or rising) during this oscillation.

6. CONCLUSIONS

Spatial measurements of the toroidal and poloidal magnetic field components have been performed in the experiment REPUTE-1, operated in the RFP mode.

When the pinch parameter, θ, was raised deliberately, the safety factor on axis, q_0, decreased until a lower limit, $q_0 \sim 0.10$, was reached, in accordance with results published in Ref. [16]. Detailed measurements of the plasma parameters near this limit, presented for the first time in this article, revealed an $m = 0$ magnetic field oscillation resulting from two alternating processes: current peaking and field relaxation. From the observation that q_0 increases during the relaxation phase and from the time history of the $m = 1$ VUV fluctuations before and after the relaxation (indicative of MHD activity), we conclude that the relaxation mechanism can, at least in part, be attributed to MHD instability, in accordance with numerical results of non-linear resistive MHD theory.

APPENDIX

In this Appendix, the fitting functions of the magnetic field are given [20]. The functions for the toroidal field $B_t(r)$ and the poloidal field $B_p(r)$, including a first order toroidal correction, are:

$$B_t(r) = B_{t0}(r - r_0) + B_{t1}(r - r_0) \tag{1}$$

$$B_p(r) = B_{p0}(r - r_0) + B_{p1}(r - r_0) \tag{2}$$

Here, r denotes the radial position (r = 0, geometrical axis). The position of the magnetic axis and the major radius are designated by r_0 and R. The plasma minor radius a is defined as

$$a_{lim} - r_0 + \Delta(a_{lim} - r_0)$$

where a_{lim} is the limiter radius (a_{lim} = 20 cm in this experiment). The Shafranov shift $\Delta(a_{lim} - r_0)$ is defined later (Eq. (7)). The functions $B_{t0}(x)$ and $B_{p0}(x)$ are defined as

$$B_{t0}(x) = \sum_{n=1}^{4} a_n x^{2n-2} \tag{3}$$

$$B_{p0}(x) = \sum_{n=1}^{4} b_n x^{2n-1} \tag{4}$$

where a_n and b_n as well as r_0 are fitting parameters. These parameters are chosen such that the toroidal and poloidal currents fall to zero at the plasma edge (at the limiter). The toroidal correction terms, B_{t1} and B_{p1}, are described with the help of B_{t0} and B_{p0} as

$$B_{t1}(r - r_0) = -\frac{r - r_0}{R} B_{t0}(r - r_0) + \Delta(r - r_0)\frac{dB_{t0}(r - r_0)}{dr} \tag{5}$$

$$B_{p1}(r - r_0) = \frac{r - r_0}{R} B_{p0}(r - r_0)\Lambda(r - r_0) + \Delta(r - r_0)\frac{dB_{p0}(r - r_0)}{dr} \tag{6}$$

where

$$\Delta(r - r_0) = \int_{r_0}^{r} \frac{r' - r_0}{R}[\Lambda(r' - r_0) + 1]dr' \tag{7}$$

The function $\Lambda(r - r_0)$ is defined as

$$\Lambda(r - r_0) = \frac{\int_{r_0}^{r}[B_{p0}(r' - r_0)]^2(r' - r_0)dr'}{[B_{p0}(r - r_0)]^2(r - r_0)^2} - 1 \tag{8}$$

The toroidal current $j_t(r)$ and the poloidal current $j_p(r)$ also contain toroidal correction terms described as

$$j_t(r) = j_{t0}(r - r_0) + j_{t1}(r - r_0) \tag{9}$$

$$j_p(r) = j_{p0}(r - r_0) + j_{p1}(r - r_0) \tag{10}$$

The zeroth order current densities are calculated as

$$j_{t0}(r - r_0) = \frac{1}{\mu_0}\frac{1}{r - r_0}\frac{d}{dr}[(r - r_0)B_{p0}(r - r_0)] \tag{11}$$

$$j_{p0}(r - r_0) = -\frac{1}{\mu_0}\frac{d}{dr}B_{t0}(r - r_0) \tag{12}$$

The first order toroidal correction terms are represented by the zeroth order terms, which are

$$j_{t1}(r - r_0) = \frac{r - r_0}{R}\left[\frac{2}{B_{p0}(r - r_0)}\frac{dp}{dr} - j_{t0}(r - r_0)\right] + \Delta(r - r_0)\frac{dj_{t0}(r - r_0)}{dr} \tag{13}$$

$$j_{p1}(r - r_0) = \frac{r - r_0}{R} j_{p0}(r - r_0)\Lambda(r - r_0) + \Delta(r - r_0)\frac{dj_{p0}(r - r_0)}{dr} \tag{14}$$

Here, $dp/dr = (j \times B)_r$. The safety factor q(r) is defined as

$$q(r) = \frac{r - r_0}{R}\frac{B_{t0}(r - r_0)}{B_{p0}(r - r_0)} \tag{15}$$

The ratio of the current density to the magnetic field λ is defined as

$$\lambda = \mu_0 \frac{\vec{j} \cdot \vec{B}}{B^2} \tag{16}$$

ACKNOWLEDGEMENTS

The authors are grateful to the members of the REPUTE-1 experimental group for their co-operation and helpful support. The authors also wish to thank Mr. K. Kusano for useful information on the resistive MHD theory.

REFERENCES

[1] BODIN, H.A.B., NEWTON, A.A., Nucl. Fusion **20** (1980) 1255.
[2] TAYLOR, J.B., Phys. Rev. Lett. **33** (1974) 1139.
[3] SYKES, A., WESSON, J.A., Phys. Rev. Lett. **37** (1976) 140.
[4] CARAMANA, E., NEBEL, R.A., SCHNACK, D., Phys. Fluids **26** (1983) 1305.
[5] SCHNACK, D., CARAMANA, E., NEBEL, R.A., Phys. Fluids **28** (1985) 321.
[6] SATO, T., KUSANO, K., Phys. Rev. Lett. **54** (1985) 808.
[7] HUTCHINSON, I.H., Plasma Phys. **26** (1984) 539.
[8] KUSANO, K., SATO, T., Nucl. Fusion **26** (1986) 1051.
[9] MIYAMOTO, K., Nucl. Fusion **25** (1985) 1677.
[10] WATT, R.G., NEBEL, R.A., Phys. Fluids **26** (1983) 1168.
[11] WURDEN, G.A., Phys. Fluids **27** (1984) 551.
[12] WATT, R.G., LITTLE, E.M., Phys. Fluids **27** (1984) 784.
[13] PHILLIPS, J., BAKER, D., BURKHARDT, L., ERICKSON, R., HABERSTICH, A., INGRAHAM, J., LITTLE, E., MELTON, J., SCHOENBERG, K., WATT, R., WEBER, P., WURDEN, G., Observations of Ramped Current Operation in ZT-40M, Res. Rep. LA-10060-MS, Los Alamos National Laboratory (1984).
[14] HIRANO, Y., KONDOH, Y., MAEJIMA, Y., NOGI, Y., OGAWA, K., SATO, M., SHIMADA, T., YAGI, Y., YOSHIMURA, H., in Plasma Physics and Controlled Nuclear Fusion Research 1984 (Proc. 10th Int. Conf. London, 1984), Vol. 2, IAEA, Vienna (1985) 475.
[15] ANTONI, V., ORTOLANI, S., in Controlled Fusion and Plasma Physics (Proc. 12th Europ. Conf. Budapest, 1985), Vol. 1, European Physical Society (1985) 582.
[16] ORTOLANI, S., in Mirror-Based and Field-Reversed Approaches to Magnetic Fusion (Proc. Workshop Varenna, 1983), Vol. 2, International School of Plasma Physics, Varenna (1984) 513.
[17] MIYAMOTO, K., INOUE, N., Nucl. Fusion **25** (1985) 1303.
[18] SCHOENBERG, K., GRIBBLE, R., PHILLIPS, J., Nucl. Fusion **22** (1982) 1433.
[19] WERLEY, K.A., NEBEL, R.A., WURDEN, G.A., Phys. Fluids **28** (1985) 1450.
[20] SHAFRANOV, V.D., Reviews of Plasma Physics, Vol. 2, Consultants Bureau, New York (1966) 103.

Manuscript received 5 May 1986
Final manuscript received 15 June 1987)